

# Oscillations in Rapid Fracture

Ariel Livne, Oded Ben-David and Jay Fineberg

*The Racah Institute of Physics, The Hebrew University of Jerusalem, Jerusalem 91904, Israel*

Experiments of pure tensile fracture in brittle gels reveal a new dynamic oscillatory instability whose onset occurs at a critical velocity,  $V_C = 0.87C_S$ , where  $C_S$  is the shear wave speed. Until  $V_C$  crack dynamics are well described by linear elastic fracture mechanics (LEFM). These extreme speeds are obtained by suppression of the micro-branching instability, which occurs when sample thicknesses are made comparable to the minimum micro-branch width. The wavelength of these sinusoidal oscillations is independent of the sample dimensions, thereby suggesting that a new intrinsic scale exists that is unrelated to LEFM.

PACS numbers: 46.50.+a, 62.20.Mk, 47.54.+r

The dynamics of rapidly moving cracks are of both fundamental and practical importance. Driven by the elastic energy stored in a stressed body, brittle cracks accelerate towards their theoretical limiting speed [1]. However in tensile fracture, the crack tip becomes unstable at less than half that velocity (Rayleigh wave speed -  $V_R$ ), sprouting small side cracks termed micro-branches [2]. At this point, the single-crack state is replaced by a multi-crack one and much of the energy flowing to the crack tip, is transformed into additional fracture surface (roughness). The density of micro-branches is observed to increase with the main crack velocity and as a consequence, cracks are rarely observed at velocities greater than  $0.6 - 0.7V_R$ .

We describe experiments performed on polyacrylamide gels. Fracture dynamics in these materials have been shown [3] to be identical to those of standard brittle amorphous materials, with the advantage that the extremely slow wave speeds in gels simplify the study of crack dynamics. We demonstrate that, when micro-branches are suppressed, crack dynamics are well-described by the single-crack equation of motion up to previously unattainable crack speeds. Surprisingly, we find that a new oscillatory instability occurs at a critical velocity close to  $V_R$ . The existence of this instability highlights important unresolved questions regarding the path selection of dynamic cracks [4, 5]. Furthermore, the suppression of micro-branches when the gel thickness approaches the process zone scale, raises interesting questions regarding both the origin of the micro-branching instability and the relevant length scale at which 3D fracture becomes effectively 2D.

Our experiments were performed using sheets of brittle polyacrylamide gels of typical size ( $X \times Y$ )  $125 \times 115 \text{ mm}^2$  and thickness  $0.15 < d < 0.35 \text{ mm}$  where X, Y and Z are, respectively, the propagation, loading, and sheet thickness directions. All experiments reported here were performed in polyacrylamide gels composed of 13.8% total monomer concentration and 2.6% bis-acrylamide as cross-linker [6]. These gels have a measured shear modulus of  $G = 35.2 \pm 1.4 \text{ kPa}$  yielding shear and longitu-

dinal wave speeds of  $C_S = 5.90 \pm 0.15 \text{ m/s}$  and  $C_L = 11.8 \pm 0.3 \text{ m/s}$ , respectively. Measurements of  $C_S$  and  $C_L$  using high-speed photography agree with these values to within  $0.1 \text{ m/s}$ . Experiments using other gel compositions (e.g., 23% total monomer concentration with 10% bis-acrylamide whose  $C_S \sim 17 \text{ m/s}$ ) exhibit similar qualitative and quantitative behavior. The gels were cast for each experiment between flat glass plates. To ensure uniformity, the evaporation of the gel's water content was limited to below 5%. We compensated for any resulting variations in wave speeds by direct measurement of  $G$  for each experiment.

The experimental setup and measurement techniques are described elsewhere [3] and will be briefly reviewed here. The gel sheets were loaded in Mode I (uniaxial extension) via constant displacement in the vertical (Y) direction. The applied force was monitored through a load cell. When a desired stress was reached, a short cut was made at the sample's edge, midway between the vertical boundaries. This seed crack either immediately or after a short creep accelerated to dynamic velocities. Throughout each experiment the crack tip's profile and immediate location were monitored by a high speed camera set to a  $X \times Y$  spatial resolution of  $1280 \times 64/96$  pixels (frame rate of  $7.2/5 \text{ kHz}$ ). At the completion of the fracture event, the fracture surface (XZ plane) was analyzed via an optical microscope and the fracture profile (XY plane) was scanned with 2400dpi resolution.

The dynamics of a typical experiment in thin gels are presented in Fig. 1a. The initial crack propagates along a straight trajectory until losing its directional stability to crack tip oscillations in the XY plane. Straight-line propagation (Fig. 1b) typical of micro-branch free fracture gives way to sinusoidal oscillations at a millimeter scale. The fracture surface formed by oscillating cracks is typically smooth (mirror-like), with rare instances of short directed lines of successive micro-branches ("branch-lines") [7]. This behavior is in contrast to propagation in thicker samples where the crack retains its straight line trajectory throughout the fracture process (Fig. 1c). In these latter events, the fracture surface is micro-branch

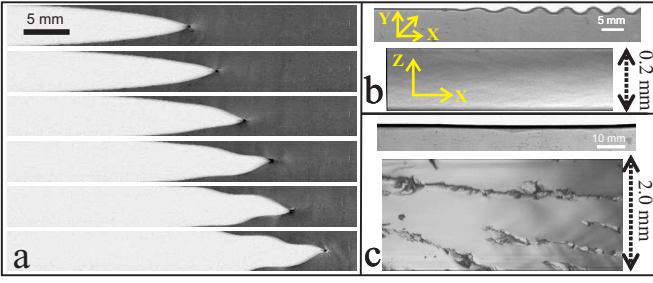


FIG. 1: (a) A sequence of photographs, shown at 0.69 ms intervals, of a propagating crack undergoing a transition from linear (top 2 pictures) to oscillatory motion. Photographs of XY profile (top) and (XZ) fracture surface (bottom) of (b) a 0.2 mm thick gel sample where oscillations developed and (c) a 2.0 mm thick gel where the crack retained its straight line trajectory. In (c) the fracture surface is micro-branch dominated whereas in (b) the oscillating crack has a mirror surface. Propagation in (a), (b) and (c) was from left to right.

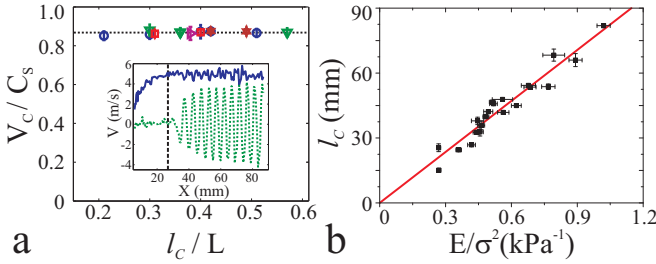


FIG. 2: (color online) (a) Oscillations appear only beyond a critical velocity of  $V_C = 0.87C_S$ .  $V_C$  is independent of the crack length at the onset,  $l_c$ , sample size,  $L$ , and thickness,  $d$ . The different symbols represent measurements for  $0.15 < d < 0.30$  mm. (inset) The velocity components,  $V_x$  (continuous line) and  $V_y$  (dotted line), as a function of  $X$ , where the dashed line marks the onset of oscillations. (b) The measured (squares) and predicted (line) relation between  $l_c$  and  $E/\sigma^2$  in the framework of LEFM [1]. The line's slope gives the fracture energy  $\Gamma(v_c) = 34 \pm 2 \text{ J/m}^2$ .

dominated; beyond a critical velocity branch-lines develop whose density increases with the crack velocity [7]. Branch-lines disappear upon arrival at the sample surfaces at  $Z=0$  or  $Z=d$ . Thus, in thin sheets branch-lines are quickly suppressed and sporadic.

The onset of the oscillations occurs at a critical velocity of  $V_C = 0.87 \pm 0.02C_S$  (Fig. 2a). The observed value of the critical velocity is independent of  $d$  for  $0.15 < d < 0.3 \text{ mm}$ . In thicker gels, cracks rarely reached  $V_C$  due to micro-branching (more on this later). Surprisingly, no evidence of the Yoffe instability [8], in which a crack is expected to deviate from its original straight line trajectory at  $V > 0.6V_R$ , is observed.

The rapid acceleration to the extreme crack velocities attained ( $V > 0.87C_S$ ) suggests that waves reflected from the system's remote boundaries can not affect crack dynamics, as reflected waves only catch up with the crack

tip well beyond the critical crack length  $l = l_c$ . Thus, for  $V \leq V_C$ , predictions by linear elastic fracture mechanics (LEFM) of the equation of motion for a single edge crack in a semi-infinite body [1] should hold:  $V = V_R(1 - \Gamma(v)E/K^2)$  where  $K = 1.12\sigma\sqrt{\pi l}$  and  $\Gamma$  is the material's fracture energy [9]. At  $V = V_C$  this predicts  $l_c$  to be:

$$l_c = \frac{\Gamma(v_c)E}{1.12^2\pi\sigma^2(1 - V_C/V_R)} \quad (1)$$

Eq. 1 predicts that  $l_c \propto \sigma^{-2}$  where  $\sigma$  is the applied stress. This prediction (Fig. 2b) is, indeed, in excellent agreement with measurements of  $l_c$ . The slope of the linear fit yields a value of the fracture energy,  $\Gamma(V_C) = 34 \pm 2 \text{ J/m}^2$ , which agrees with previous measurements [10]. The slight scatter in Fig. 2b is consistent with our 5% allowed variation of  $G$ . This is the first direct experimental verification of the equation of motion of a single crack at velocities approaching  $V_R$  [11].

At  $V_C$  the behavior of the crack's two velocity components,  $V_x$  and  $V_y$ , changes abruptly. Prior to  $V_C$ ,  $V_y = 0$  whereas beyond  $V_C$ ,  $V_y$  oscillates at a wavelength,  $\lambda(x)$ , with increasing amplitude. The oscillations in  $V_y$  are accompanied by a much smaller oscillatory component of  $V_x$  having a wavelength of  $\lambda/2$  and a  $\pi/2$  relative phase shift. (Fig. 2a inset). This suggests that  $V = \sqrt{V_x^2 + V_y^2}$  does not, itself, oscillate but increases monotonically, although we lack the temporal resolution to directly verify this.

$V_x$  increases steadily until reaching  $V_C$ . Beyond  $V_C$ , the full velocity,  $V$ , generally continues to accelerate (see e.g. Fig. 3) to steady state velocities.  $V$ , however, has not been observed to surpass  $C_S$  [12]. Unexpectedly, the mean value, over an oscillation period, of  $V_x$  remains nearly constant (even dropping by a few percent) upon reaching  $V_C$ . This is illustrated in Fig. 3 (inset) where measured values of  $V$  are identical to values obtained by integrating the measured path length of the crack and assuming that  $V_x$  is constant, equal to its mean value for  $V > V_C$  [13].

Let us consider the nature of the oscillations. The oscillations are generally sinusoidal except for large amplitude states at the highest values of applied stress,  $\sigma$ . Both the oscillation amplitude,  $A$ , and wavelength,  $\lambda$ , develop with crack advance until reaching steady-state values after a number of cycles (Fig. 4 insets). The steady-state values of both  $A$  and  $\lambda$  vary with  $\sigma$ , as shown in Fig. 4, and do not appear to be well-defined functions of  $V$ . At  $V = V_C$ ,  $A$  initiates from a finite value, although no hysteresis in the transition to the oscillatory state has been observed.  $\lambda$  is a sharply decreasing function of  $\sigma$ . Steady-state wavelengths range from 4-9mm with  $V_x/\lambda \sim 0.5 - 1 \text{ kHz}$ . This frequency scale corresponds to the same ( $\sim 1 \text{ ms}$ ) timescale that was previously observed for micro-branching activation times in similar gels [3].

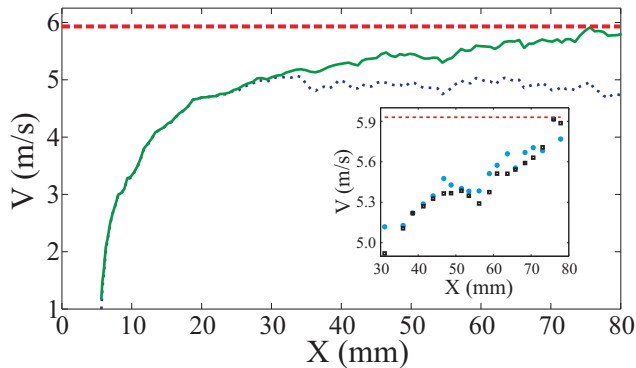


FIG. 3: (color online) The full crack velocity,  $V$  (continuous line), is compared to  $V_x$  (dotted line). Beyond  $V_C$ ,  $V$  until  $C_S$  (dashed line) [12], while  $V_x$  stays nearly (inset) A comparison of direct measurements of  $V$  (full circles) with  $V$ , calculated using the spatial transfer of the oscillations (squares) [13]. The dashed line denotes  $C_S$ . All velocities are averaged over an oscillation period.

The origin of these length/frequency scales is currently unknown. The time scale is over an order of magnitude smaller than any possible resonance with the system's boundaries. In fact, these scales are wholly *independent* of any of the physical dimensions of the sample, since gels of substantially different widths and dimensions all fall on the same steady-state amplitude/wavelength curve (Fig. 4). Furthermore, as indicated by Fig. 2b, the crack is effectively travelling in a semi-infinite medium at the onset of oscillations and, under semi-infinite conditions, the crack will have no knowledge of the actual size of the sample. We, therefore, surmise that the length scale must have its origins in an intrinsic scale, such as the process zone, that is not quantitatively accounted for in current theoretical frameworks.

Although the steady-state values of  $\lambda$  and  $A$  are well-defined, their initial transients (Fig. 4 - insets) are extremely diverse, with no discernable relation to either  $V$  or  $\sigma$ . It is interesting, however, that these transients follow a number of distinct  $A - \lambda$  trajectories, suggesting that there may be a number of meta-stable solution branches that eventually evolve to the steady-states presented in Fig. 4.

Why is the oscillatory instability not readily observed in thick samples? Basically, in thick samples cracks rarely attain  $V_C$ , due to the onset of micro-branching. Let us momentarily digress and consider the relation of micro-branch formation to sample thickness. Recent work in gels indicates that the micro-branching instability is a first-order phase transition in which micro-branch formation is triggered by noise, above a critical velocity [3]. Micro-branches in gels have a minimal width [3],  $\Delta Z$ , whose scale (here  $\sim 40\mu\text{m}$ ) is approximately that of the process zone. The system's quenched noise level may then be related to  $d/\Delta Z$ . This may explain why the

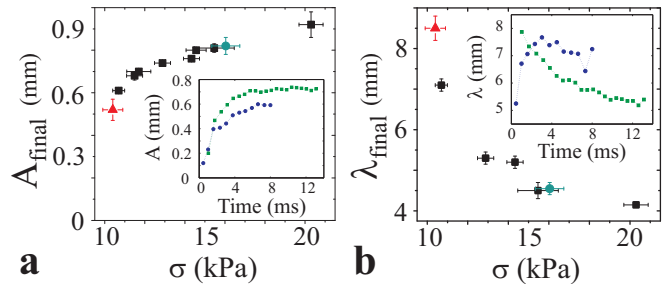


FIG. 4: (color online) Steady-state amplitudes,  $A$ , (a) and wavelengths,  $\lambda$ , (b) as a function of the applied stress,  $\sigma$ . (insets) Transient time evolution of  $A$  and  $\lambda$  in two typical experiments.  $t=0$  defines the onset of oscillations. Sample dimensions:  $(X \times Y) \sim 125 \times 115\text{mm}^2$  (■),  $130 \times 155\text{mm}^2$  (▲) and  $125 \times 70\text{mm}^2$  (●).

number of branching events is strongly suppressed with decreasing  $d$ . This suppression, coupled with the disappearance of branch-lines with their arrival at the sample faces at  $Z = 0$  or  $d$  (see e.g. Fig. 1c), causes the increasingly sporadic appearance of micro-branches as  $d \rightarrow \Delta Z$ . Thus for  $d \rightarrow \Delta Z$  ( $\Delta Z \sim \mu\text{m}$  for PMMA and less for glass) micro-branching events are rare with crack dynamics becoming effectively two-dimensional. This suppression of micro-branches explains how oscillations are so easily obtained for  $d \sim 0.15 - 0.2\text{mm}$ .

Although rare, the micro-branching instability is observed in thin sheets both in straight and oscillatory propagation. When excited, micro-branches reduce the energy available to the main crack [2], and consequently reduce the main crack's velocity. If  $V$  falls below  $V_C$ , oscillations immediately cease, and the crack propagates along a straight trajectory (e.g. Fig. 5 in the 2nd shaded region). When micro-branching is sporadic, micro-branches only momentarily reduce  $V$  to below  $V_C$ . This not only causes discontinuities in the oscillation phase but before and after a velocity drop we often observe entirely different sinusoidal solutions (with significantly different wavelength and amplitude). When *prolonged* micro-branching occurs, as characteristic of the thicker gels,  $V$  only momentarily surpasses  $V_C$  between micro-branching events. In this case, pronounced "stair-case" profiles are created by momentary diversions of the crack for less than a period followed by straight line trajectories. All of these effects are demonstrated in the single experiment, presented in Fig. 5, in which  $d$  is tapered as a function of  $X$ . The rarity of micro-branches in the initial stage ( $d < 0.35\text{mm}$ ) enables rapid acceleration to  $V > V_C$  and the onset of oscillations. As the taper widens, micro-branching occurs; first sporadically (2nd shaded region) and later with prolonged branching (for  $d > 0.35\text{mm}$ ), leading to stair-case profiles.

In recent years, two oscillatory instabilities of cracks traveling in thin sheets have been reported. Both of these are fundamentally different from the oscillatory instabil-

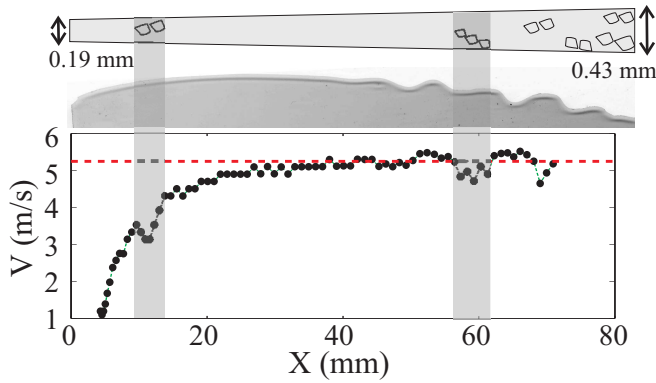


FIG. 5: (color online) Tapering of  $d$  ( $0.19 < d < 0.43\text{mm}$ ) as a function of  $X$  enables  $V > V_C$  for thicknesses ( $d > 0.35\text{mm}$ ) normally dominated by micro-branches. (top) Schematic drawing of the XZ fracture surface indicating branch-line locations and  $d(x)$ . (center) Photograph of the crack profile along the XY plane with (bottom) the corresponding velocity profile. Shaded rectangles indicate regions of sporadic branch-lines (diamond shapes at top) and the resulting drops in  $V$  until their disappearance when the branch-line encounters the  $Z = 0$  or  $d$  planes. When  $V < V_C$  ( $V_C$  denoted by the dashed line) oscillations cease with no hysteresis and cracks continue along a straight-line trajectory (e.g. second shaded region). Prolonged branching ( $d > 0.35\text{mm}$ ) yields “staircase” profiles.

ity presented here. Deegan and coworkers have observed wavy cracks traveling at intersonic velocities in biaxially-stretched thin rubber sheets [14]. In our experiments, oscillations are observed at clearly *subsonic* velocities in pure uniaxial tension. Phase field models [15], which do yield subsonic oscillations of crack trajectories, predict  $\lambda$  to scale with the system size, also in sharp contrast with our results. Recent calculations [16], pairing LEFM with the Hodgdon and Sethna [4] path selection criterion, predict the onset of oscillatory instability at close to our measured values of  $V_C$ . In contrast to our measurements however,  $\lambda$  is predicted to scale with the system size.

Oscillatory cracks have also been observed when a rigid cutting tool is forced through a thin elastic sheet [17]. These cracks travel at  $V \ll C_S$  with out-of-plane bending playing an important role. In contrast, the instability presented here is in pure Mode I with no measurable out-of-plane deflection [18]. Our oscillations are triggered at  $V_C$  values that are near  $C_S$ , irrespective of the sample’s thickness. In addition, the crack dynamics in our experiments are consistent with the single-crack (Mode I) equation of motion predicted by LEFM until either  $V_C$  or the onset of micro-branching. We therefore conclude that these observations indicate a previously unobserved instability in dynamic fracture whose characteristic time/length suggests that a new *intrinsic* scale is important to describe these dynamics. This time/length scale can not be explained in the framework of LEFM [16], underlining the necessity for a more fundamental

theoretical description of the near vicinity of the crack tip.

This research was supported by the Israel Science Foundation (grant 194/02).

- 
- [1] L. B. Freund, *Dynamic Fracture Mechanics* (Cambridge University Press, Cambridge, 1990).
  - [2] E. Sharon and J. Fineberg, Phys. Rev. B. **54**, 7128 (1996).
  - [3] A. Livne, G. Cohen and J. Fineberg, Phys. Rev. Lett. **94**, 224301 (2005).
  - [4] J. Hodgdon and J. Sethna, Phys. Rev. B. **47**, 4831 (1993).
  - [5] M. Marder, Europhys. Lett. **66**, 364 (2004); G. E. Oleaga, J. Mech. Phys. Solids **49**, 2273 (2001).
  - [6] The Acrylamide solution contains 0.02% of *NaCl* and  $\sim 60$  PPM Bromophenol blue to facilitate visualization. Polymerization is initiated by adding 0.12% APS and 0.06% TEMED. Concentrations are given here in: weight/total volume.
  - [7] E. Sharon, G. Cohen and J. Fineberg, Phys. Rev. Lett. **88**, 085503 (2002).
  - [8] E. H. Yoffe, Philos. Mag. **42**, 739 (1951).
  - [9] B. Lawn, *Fracture of Brittle Solids - Second Edition* (Cambridge University Press, Cambridge, 1993).
  - [10] Y. Tanaka, K. Fukao and Y. Miyamoto, Eur. Phys. J. E. **3**, 395 (2000); T. Baumberger, C. Caroli and D. Martina, Nature Mat. **5**, 552 (2006).
  - [11] E. Sharon and J. Fineberg, Nature **397**, 333 (1999).
  - [12] The limiting velocity should be  $V_R = 0.955C_S$  and not  $C_S$ . In a number of experiments, the crack’s maximal velocity was between  $V_R$  and  $C_S$ . This discrepancy might be due to measurement accuracy ( $\sim 3\%$ ) or a different form for  $V_R$  in elastomers/ thin sheets.
  - [13] From post-mortem XY scans of the gels, we measure  $\lambda$  and  $A$  for each period. The corresponding length of the crack’s path is:  $l = \lambda \cdot F(A/\lambda)$ . Defining  $\bar{V}$  and  $\bar{V}_x$  as the mean values of  $V$  and  $V_x$  over one period ( $T$ ) we find:  $\bar{V} = l/T$  and  $\bar{V}_x = \lambda/T$ . Therefore  $\bar{V}/\bar{V}_x = F(A/\lambda)$  where  $F$  is solved numerically.
  - [14] R. D. Deegan *et al.*, Phys. Rev. Lett. **88**, 014304 (2002); P. J. Petersan *et al.*, Phys. Rev. Lett. **93**, 015504 (2004).
  - [15] H. Henry and H. Levine, Phys. Rev. Lett. **93**, 105504 (2004); A. Karma and A. E. Lobkovsky, Phys. Rev. Lett. **92**, 245510 (2004).
  - [16] E. Bouchbinder and I. Procaccia, companion Letter.
  - [17] A. Ghatak and L. Mahadevan, Phys. Rev. Lett. **91**, 215507 (2003); B. Roman *et al.*, C. R. Mécanique **331**, 811 (2003).
  - [18] The relevance of mode III fracture to these oscillations was ruled out in the following manner: With a laser sheet we illuminated a thin line on the gel which was oriented parallel to the Y axis at a point midway along the X axis, where (future) crack oscillations appear. If the crack tip opening in the vicinity of this line were in mode III, we would expect to observe deflection of the line, when traversed by the crack. No such deflection was observed to the  $< 5^\circ$  measurement accuracy.